

## Infrared spectroscopy of amorphous hydrogenated GaAs: Evidence for H bridges

Z. P. Wang,\* L. Ley, M. Cardona

*Max-Planck-Institut für Festkörperforschung, Heisenbergstrasse 1,  
7000 Stuttgart 80, Federal Republic of Germany*

(Received 8 March 1982)

The infrared absorption spectra of hydrogenated amorphous GaAs show two prominent hydrogen-related bands at 530 and 1460  $\text{cm}^{-1}$ . These bands are very broad and they amount to most of the hydrogen-induced infrared absorption. The remaining structures are a number of comparatively sharp lines which we interpret as Ga-H and As-H modes in partial agreement with earlier investigations. We argue that the broad bands arise from near-stretching (1460  $\text{cm}^{-1}$ ) and from wagging (530  $\text{cm}^{-1}$ ) vibrations of H atoms situated in bridging positions between two Ga atoms. This assignment is supported by similar bands in Al-H polymers, *a*-GaP:H, and *a*-GaSb:H. A model calculation of the mode frequencies is also presented.

### INTRODUCTION

Hydrogenated amorphous GaAs (*a*-GaAs:H) has been successfully prepared by rf sputtering in an Ar-H<sub>2</sub> mixture.<sup>1</sup> The electrical and optical properties of *a*-GaAs:H have been investigated.<sup>1-4</sup> The effect of H addition shifts the optical absorption edge to higher energies and decreases the conductivity by several orders of magnitude. It also produces some infrared absorption bands related to Ga-H and As-H bonds. These phenomena show that the incorporation of H into *a*-GaAs can compensate dangling bonds and reduce the density of states in the energy gap. However, no non-linearity or rectification has been observed in *a*-GaAs:H Schottky barriers.<sup>2</sup> This is probably due to either a large bulk defect density or to a large density of surface states.

Paul *et al.*<sup>3</sup> have presented infrared vibrational spectra of *a*-GaAs:H. These spectra appear to be composed of two very broad and strong bands and some other weak bands. The spectra seem more complex than in the case of *a*-Si:H and *a*-Ge:H. In this paper we present further details about the infrared spectra of *a*-GaAs:H. The infrared spectra of *a*-GaP:H and *a*-GaSb:H are also presented and compared with those of *a*-GaAs:H. The broad features mentioned above are also observed for *a*-GaP:H and *a*-GaSb:H. They are interpreted in terms of Ga-H-Ga bridging bonds.

### PREPARATION AND CHARACTERIZATION OF THE AMORPHOUS SAMPLES

The samples were prepared by rf sputtering of a polycrystalline GaAs target of 2-in. diameter in an Ar:H<sub>2</sub> mixture. The distance between target and substrate was 5 cm, the substrate was grounded, and the rf power applied to the target was 40–80 W. The base pressure was about  $2 \times 10^{-6}$  Torr. The Ar pressure ( $p_{\text{Ar}}$ ) was maintained at  $1 \times 10^{-2}$  Torr, but the partial pressure of H<sub>2</sub> ( $p_{\text{H}}$ ) was varied between 0 and  $1 \times 10^{-2}$  Torr. The deposition rate was about 0.2–0.6  $\mu\text{m}/\text{h}$ . The thickness of films ranged from 2–8  $\mu\text{m}$ . The films were deposited simultaneously on various substrates including fused quartz, glass, and *c*-Si. The substrate temperature  $T_s$  was held at about 20°C by means of cooled water in order to obtain the amorphous phase of GaAs. X-ray diffraction showed that the films are indeed amorphous. Partially crystalline films can be obtained if the cooling water is cut off, especially for the higher rf power. Paul *et al.*<sup>3</sup> pointed out that if the substrate temperature is held near 4°C amorphous films are obtained. Temperatures above 40°C result in crystalline films. Hargreaves *et al.*,<sup>2</sup> however, believe that amorphous GaAs films result for temperatures between 20 and 30°C. Some polycrystalline GaAs films were produced at substrate temperature of 200°C. The Raman spec-

trum provides a fast and convenient method to identify whether the film is amorphous or partially crystalline.<sup>5</sup> Figure 1 shows Raman spectra in the region of the optical phonons of *a*-GaAs:H films prepared at different  $T_s$ . At the lower  $T_s$  these Raman spectra appear as a broad band centered at  $250\text{ cm}^{-1}$ . With increasing  $T_s$ , this band shifts to higher energies and the line width is reduced. For  $T_s$  larger than  $\sim 50^\circ\text{C}$  the Raman spectra split into two peaks which correspond to the TO and LO phonons of *c*-GaAs, and partially crystalline films result.

### EXPERIMENTAL RESULTS

The infrared transmission spectra from  $4000$  to  $200\text{ cm}^{-1}$  of a set of samples deposited on *c*-Si substrates at different  $P_H$  were measured with a Perkin-Elmer model 283 double-beam spectrophotometer with a blank *c*-Si substrate in the reference beam. The absorption coefficient  $\alpha$  was calculated from the measured transmittance  $T$  according to the following equation<sup>6</sup>:

$$\alpha = -\frac{1}{t} \ln \frac{1}{B} \{A + [A^2 + 2BT(1 - R_2R_3)]^{1/2}\},$$

$$A = -(1 - R_1)(1 - R_2)(1 + R_3), \quad (1)$$

$$B = 2T(R_1R_2 + R_1R_3 - 2R_1R_2R_3),$$

where  $t$  is the thickness of the film, and  $R_1$ ,  $R_2$ ,

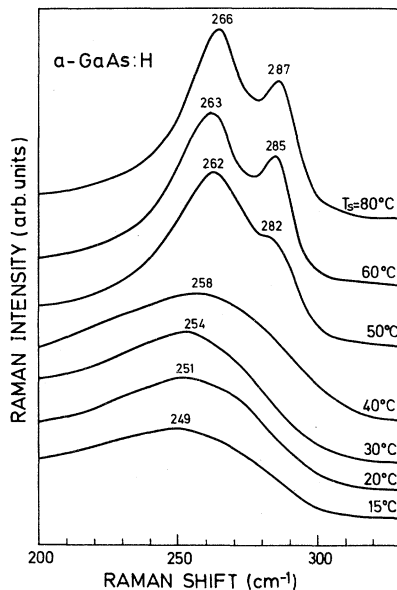


FIG. 1. Raman spectra of *a*-GaAs:H prepared at the different  $T_s$ .

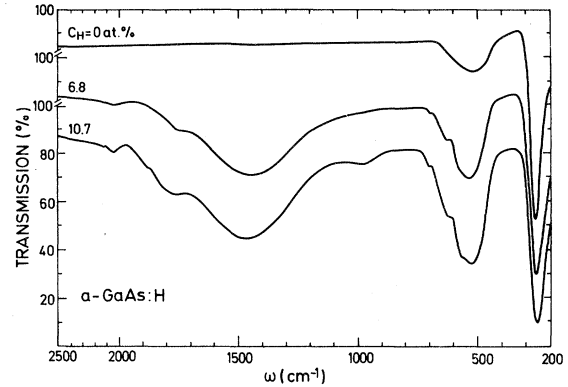


FIG. 2. Infrared transmission spectra of *a*-GaAs:H with different  $C_H$ .

and  $R_3$  are reflectance of the air-film, film-substrate, and substrate-air interfaces, respectively. Figure 2 shows the infrared transmission spectra of *a*-GaAs with  $C_H = 0, 6.8$ , and  $10.7$  at. %. Figure 3 shows the corresponding absorption spectrum of *a*-GaAs:H with  $C_H = 10.7$  at. % and the decomposition into separate lines. The broad hump at  $520\text{ cm}^{-1}$  represents the contribution from the 2TO band. Its intensity relative to the TO band at  $255\text{ cm}^{-1}$  was deduced from the spectrum of *a*-GaAs without hydrogen. For the remainder of the lines (except the band at  $1460\text{ cm}^{-1}$ ) symmetrical Lorentzians have been superimposed to reproduce the measured spectrum. Figure 4 shows the infrared transmission spectra of *a*-GaAs:H prepared with  $P_H = 5 \times 10^{-3}$  Torr and *a*-GaAs:D with  $p_D = 5 \times 10^{-3}$  Torr. After these measurements, the samples were isochronally annealed in vacuum ( $2 \times 10^{-5}$  Torr) for 1 h at several temperatures.

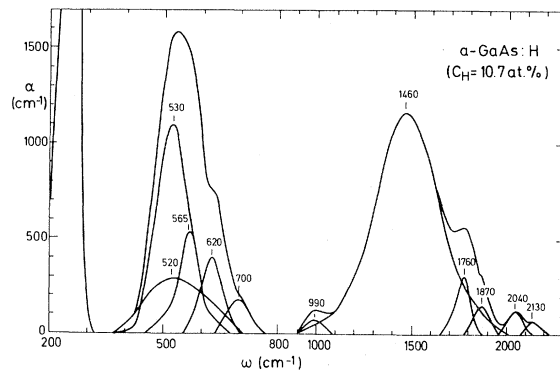


FIG. 3. Infrared absorption spectra of *a*-GaAs:H with  $C_H = 10.7$  at. %, together with the constituting lines. For an identification of the corresponding modes, compare Table I.

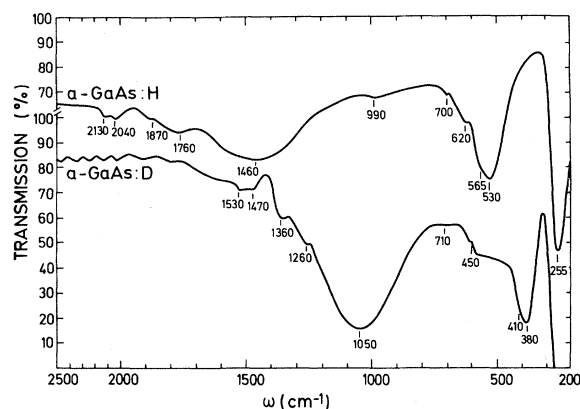


FIG. 4. Infrared transmission spectra of *a*-GaAs:H and *a*-GaAs:D.

Figures 5, 6, and 7 show the infrared, Raman, and x-ray diffraction spectra after annealing at  $T_a$ . It can be roughly estimated from Fig. 5 that hydrogen has nearly completely evolved at about 300°C (the band left at  $\sim 520$  cm $^{-1}$  after annealing at 300°C is the first overtone of the intrinsic TO band). At the same temperature, amorphous GaAs starts to recrystallize as shown in Figs. 6 and 7: X-ray diffraction exhibits two weak and broad humps below  $T_a = 250^\circ\text{C}$ , but above  $T_a = 275^\circ\text{C}$  three characteristic diffraction peaks, corresponding to the (111), (220), and (311) reflections in polycrystalline GaAs, appear. This is similar to the case of *a*-Si:H (Ref. 7) although the crystallization temperature of *a*-GaAs is closer to that of *a*-Ge. The change of the corresponding Raman spectra

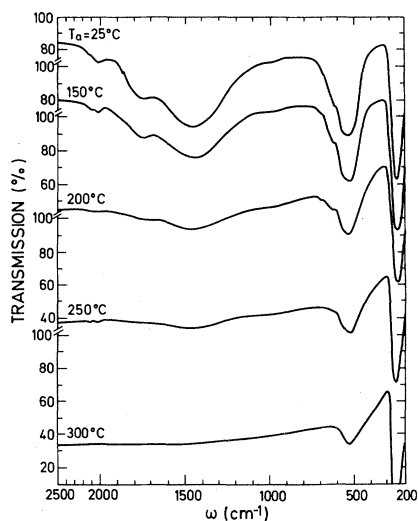


FIG. 5. Infrared transmission spectra of *a*-GaAs:H after thermal annealing at the different  $T_a$ .

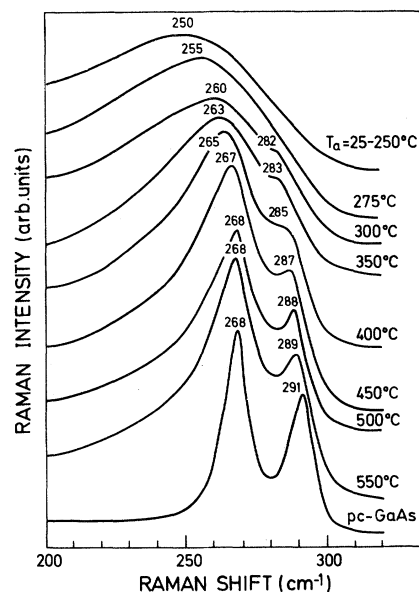


FIG. 6. Raman spectra of *a*-GaAs:H after thermal annealing at the different  $T_a$ .

with annealing temperature  $T_a$  is shown in Fig. 6. Above  $T_a = 300^\circ\text{C}$  the Raman spectra split into two peaks which shift to higher energy with increasing  $T_a$ . We can estimate that the recrystallization of *a*-GaAs:H occurs in the annealing temperature range 270–300°C.

The wave numbers of the characteristic ir-absorption peaks observed in *a*-GaAs:H are given in Fig. 3. There is a weak doublet at 2040 and 2130 cm $^{-1}$ . We assign these peaks to AsH and AsH $_2$  stretching modes, respectively, by comparison with the infrared spectra of arsenic hydrides.<sup>8</sup> For our deposition conditions the peak at 2040

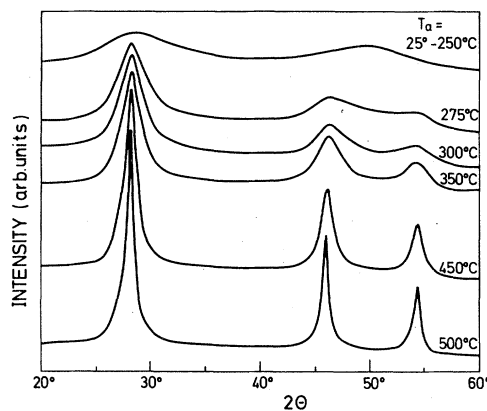


FIG. 7. X-ray diffraction spectra of *a*-GaAs:H after thermal annealing at the different  $T_a$ .

$\text{cm}^{-1}$  is always dominant. However, with increasing  $p_{\text{H}}$  the relative intensity of the peak at  $2130 \text{ cm}^{-1}$  increases significantly, as shown in Fig. 8. After annealing the  $\text{AsH}_2$  stretching mode increases strength with respect to the  $\text{AsH}$  stretching mode with increasing  $T_a$ , as shown in Fig. 9. This behavior is very similar to that of the  $\text{GeH}$  and  $\text{GeH}_2$  stretching modes in  $a\text{-Ge:H}$ .<sup>9</sup> These peaks have their counterparts in the deuterated samples at  $1530$  and  $1470 \text{ cm}^{-1}$ .

In the hydrogenated samples there is also a peak at  $1760 \text{ cm}^{-1}$  and a shoulder at  $1870 \text{ cm}^{-1}$ . The structures are not always very clear as they are superimposed on a very broad and strong peak which will be discussed below. We identify them as  $\text{GaH}$  and  $\text{GaH}_2$  stretching modes by comparison with the infrared spectra of some gallium hydrides.<sup>10,11</sup>

Note that the  $\text{Ga-H}$  and  $\text{As-H}$  stretching modes are symmetrically disposed with respect to the  $\text{Ge-H}$  frequencies,<sup>9</sup> as expected. For our deposition conditions, the peak at  $1760 \text{ cm}^{-1}$  is always dominant. The shoulder at  $1870 \text{ cm}^{-1}$  is very weak and can be only observed for the higher  $p_{\text{H}}$ . In  $\text{GaAs:D}$  the  $\text{GaD}_2$  stretching mode at  $1360 \text{ cm}^{-1}$  is stronger, while the  $\text{GaD}$  stretching mode at  $1260 \text{ cm}^{-1}$  is somewhat weaker.

By comparison with the infrared spectra of other arsenic and gallium hydrides<sup>8,10,11</sup> and with the position of the bond-bending modes in  $a\text{-Si:H}$  (Ref. 12) and  $a\text{-Ge:H}$  (Ref. 9) we assign two peaks observed at  $990$  and  $700 \text{ cm}^{-1}$  to  $\text{As-H}_2$  and  $\text{Ga-H}_2$  bending modes, respectively.

In view of its large strength as compared with the modes described so far, we do not attribute the

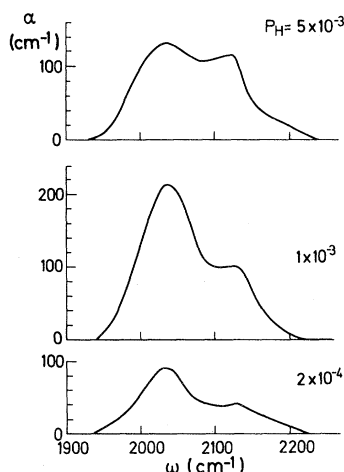


FIG. 8. Infrared absorption spectra of  $\text{As-H}$  stretching modes for the different  $p_{\text{H}}$  (in Torr).

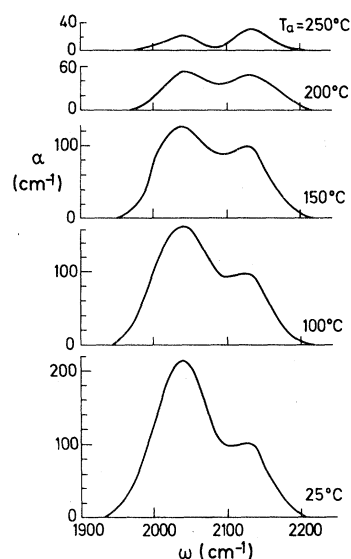


FIG. 9. Infrared absorption spectra of  $\text{As-H}$  stretching modes for the different  $T_a$  ( $p_{\text{H}} = 1 \times 10^{-3}$  Torr).

peak at  $530 \text{ cm}^{-1}$  in  $a\text{-GaAs:H}$  to bond wagging vibrations. We believe that the standard wagging modes in  $a\text{-GaAs:H}$  appear only as two shoulders, one at  $620 \text{ cm}^{-1}$  for the wagging mode of the  $\text{As-H}$  bond, and another at  $565 \text{ cm}^{-1}$  for that of  $\text{Ga-H}$ .

As already mentioned, there are two strong and broad bands at  $1460$  and  $530 \text{ cm}^{-1}$ . Paul *et al.*<sup>3</sup> have pointed out that they are indeed hydrogenic modes. They account for most of the hydrogen-induced infrared absorption in  $a\text{-GaAs:H}$ . We assign them to  $\text{Ga-H-Ga}$  bridge stretching and wagging modes, respectively, and will discuss them further in the following section. All the modes observed and their assignments are listed in Table I. For comparison the results of Paul *et al.*<sup>3</sup> and data for other related materials are also listed in this table. The frequency ratio of the corresponding modes in  $a\text{-GaAs:H}$  and  $a\text{-GaAs:D}$  lies between  $1.38$  and  $1.39$ , only slightly weaker than the square root of the corresponding mass ratio ( $1.41$ ). The defect in the mass ratio is most likely due to bond anharmonicity.<sup>13</sup> We point out that the anomalously low frequency ratio ( $1.30$ ) found by Lüth and Matz<sup>13</sup> for the stretching modes of  $\text{As-H(D)}$  on  $c\text{-GaAs}$  surfaces does not appear here. Although we do not know the reason for this discrepancy, we point out that the  $\text{As-D}$  stretching frequency of Ref. 13 is out of line with those reported here, while in all other cases the results of Ref. 13 agree within error with the ones observed

TABLE I. Energies (in  $\text{cm}^{-1}$ ) and identification of the vibrational modes in  $\alpha$ -GaAs:H.

$\alpha$ -GaAs:H	2130	2040	1870	1760	1460	990	700	620	565	530	520	255
	As-H <sub>2</sub> str. <sup>a</sup>	As-H str.	Ga-H <sub>2</sub> str.	Ga-H str.	Ga-H-Ga str.	As-H <sub>2</sub> bend <sup>b</sup>	Ga-H <sub>2</sub> bend	As-H wag <sup>c</sup>	Ga-H wag	Ga-H-Ga wag	2TO	TO
$\alpha$ -GaAs:D	1530	1470	1360	1260	1050	710		450	410	380		
$\omega_{\text{H}}/\omega_{\text{D}}$	1.39	1.39	1.38	1.40	1.39	1.39		1.38	1.38	1.39		
$\alpha$ -GaAs:H <sup>d</sup>	2135	2060		1780	1480	1008	840			530	258	TO
	As-H str.	As-H str.		Ga-H str.	hydro- genic mode (str.)	As-H bend	hydro- genic mode bend			2TO + hydro- genic mode		
AsH <sub>4</sub> Br <sup>e</sup> (145 K)	2174	2119				1002	836					
	As-H str.	As-H str.				As-H bend	As-H bend					
AsH <sub>3</sub> <sup>e</sup> (82 K)	2092					975	895					
	As-H str.					As-H bend	As-H bend					
NaGaH <sub>4</sub> <sup>f</sup>			1755	1750			720	575				
			Ga-H str.	Ga-H str.			Ga-H bend	Ga-H bend				
(CH <sub>3</sub> ) <sub>3</sub> PGaH <sub>3</sub> <sup>g</sup>			1832	1808			765	690	498			
			str. sym.	str. asym.			GaH <sub>3</sub> asym. sym.	GaH <sub>3</sub> bend	GaH <sub>3</sub> rock			
GaAs <sup>h</sup> (100) sur- face adsorbed H	2150		1890									
	As-H str.		Ga-H str.									
GaAs <sup>h</sup> (100) sur- face adsorbed D	1660		1380									
	? (see text)		Ga-D str.									
GaAs <sup>i</sup> H Ion Implantation			1840									
			Ga-H str.									

<sup>a</sup>Stretching mode.<sup>b</sup>Bending mode.<sup>c</sup>Wagging mode.<sup>d</sup>Reference 3.<sup>e</sup>Reference 8.<sup>f</sup>Reference 10.<sup>g</sup>Reference 11.<sup>h</sup>Reference 13.<sup>i</sup>Reference 20.

by us for the Ga—H<sub>2</sub>, Ga—D<sub>2</sub>, and As—H<sub>2</sub> bonds, respectively. It is also worth mentioning that for H on the surface of *c*-Si, the Si-H peaks occur  $\sim 100\text{ cm}^{-1}$  higher than for Si-H in *a*-Si and near those of Si-H<sub>2</sub> for this material.<sup>14</sup> Hence the peaks observed in Ref. 13, with the possible exception of that at  $1660\text{ cm}^{-1}$ , are probably those of singly bonded H and D.

## DISCUSSION

The possible existence of hydrogen bridges (sometimes called three-center bonds or simply hydrogen bonds) in *a*-Si:H has been suggested by Fisch and Licciardello.<sup>15</sup> These authors conjectured that the residual density of states in the gap of *a*-Si:H (with the dangling bonds passivated by H) was due to such hydrogen bridges. Thus the possibility appeared of avoiding these states by using fluorine instead of H for saturating dangling bonds. To date, however, no evidence for such bridging hydrogen in either *a*-Si or *a*-Ge has been found. The reason is probably that a Si—H—Si bridge must be occupied by three electrons of which two are bonding and one is nonbonding. The nonbonding electron destabilizes the bridge and transforms it into a strongly asymmetric bridge, hardly distinguishable from an ordinary saturated dangling bond.

Let us now consider the possibility of a hydrogen atom bonded as a bridge between two Ga atoms in GaAs. The static charge of Ga in GaAs is  $\sim +1$  (atomic units).<sup>16</sup> Hence the two Ga atoms forming the bridge contribute *one electron* less than in the case of Si bonds (there are 2 electrons per atom, i.e., 0.5 per tetrahedral hybrid, two hybrids contribute to the bond). Hence now only bonding electrons participate in the hydrogen bridge, half coming from each of the Ga atoms and the rest from the 1s electron of H. The chances for stability are considerably improved. Indeed, bridging hydrogens have been found recently in a number of

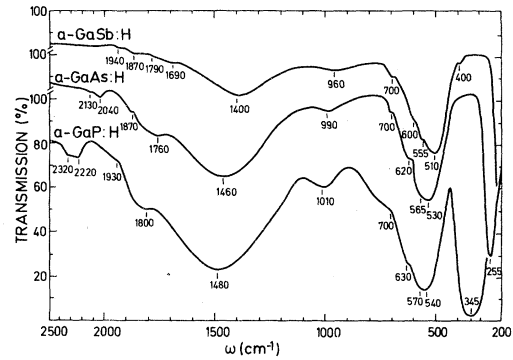


FIG. 10. Infrared transmission spectra of *a*-GaP:H ( $P_H = 2 \times 10^{-3}$  Torr,  $t = 6.6\text{ }\mu\text{m}$ ), *a*-GaAs:H ( $P_H = 1 \times 10^{-3}$  Torr,  $t = 3.8\text{ }\mu\text{m}$ ), and *a*-GaSb:H ( $P_H = 1 \times 10^{-3}$  Torr,  $t = 7.7\text{ }\mu\text{m}$ ).

aluminum compounds (Al—H—Al bridges) such as  $\text{Al}(\text{BH}_4)_2\text{H}$  and  $\text{Al}(\text{BH}_4)_3\text{H}_2$ .<sup>17</sup> The “signature” of such bridging bonds is, as usual,<sup>18</sup> the lowering of the frequencies of the Al-H stretching vibrations as compared with the monomer bonds. For the aluminum compounds just mentioned<sup>17</sup> the Al-H-Al stretching vibrations appear as a *broad band* (another characteristic of bridging hydrogen) between  $1200$  and  $2200\text{ cm}^{-1}$ , centered near  $1650\text{ cm}^{-1}$ . We also note that diborane ( $\text{B}_2\text{H}_6$ ) is a prototype of a bridging hydrogen bond, while B belongs to the same column of the Periodic Table as Al and Ga.

The analogy between these Al-H stretching bands and the ones seen in Figs. 2, 3, 4, and 10 around  $1460\text{ cm}^{-1}$  is quite striking. It is clear that the latter are due to Ga—H as they are observed in *a*-GaP:H, *a*-GaAs:H, and *a*-GaSb:H (see Table II.) Moreover, they shift in the appropriate way when H is replaced by D. The shift from  $1650$  to  $1460\text{ cm}^{-1}$  in going from the Al—H bonds to the Ga—H bonds is also reasonable and can be explained as due to the 7% smaller covalent radius  $r_c$  of Al as compared with Ga (the vibrational frequency<sup>19</sup> should be approximately proportional to

TABLE II. Comparison of the vibrational mode frequencies (in  $\text{cm}^{-1}$ ) in *a*-GaP:H, *a*-GaAs:H, and *a*-GaSb:H.

	<i>a</i> -GaP:H	2320	2220	1930	1800	1480	1010	700	630	570	540	700	345
	<i>a</i> -GaAs:H	2130	2040	1870	1760	1460	990	700	620	565	530	520	255
	<i>a</i> -GaSb:H	1940	1870	1790	1690	1400	960	700	600	555	510	400	
												2TO	TO
Assignment	P	P					P		P				
	As-H <sub>2</sub>	As-H	Ga—H <sub>2</sub>	Ga—H	Ga—H—Ga		As-H <sub>2</sub>	Ga—H <sub>2</sub>	As-H	Ga—H	Ga—H—Ga		
	Sb	Sb					Sb		Sb				
	str.	str.	str.	str.	str.		bend	bend	wag	wag	wag		

$r_c^{-1.5}$ ; the "stretching" frequency of the bridging hydrogen in diborane is  $2050 \text{ cm}^{-1}$ ). In view of the high volatility of As, it is reasonable to assume that the hydrogen bridges connect Ga atoms which otherwise would produce a "wrong" Ga—Ga bond as a result of an As deficiency. It has been recently shown that H and D also bond preferentially to Ga in proton- and deuterium-implanted crystalline GaAs and GaP.<sup>20</sup> In this work, however, no evidence for hydrogen bridges in *c*-GaAs:H and *c*-GaP:H was seen.

It is easy to account for the main features of the 1460 and the 530 bands of the bridging hydrogen with a simple geometrical model and thereby to obtain some semiquantitative information about the structure of these bonds. We first estimate the Ga-H distance  $d_{\text{Ga-H}}$  in the hydrogen bridges. The corresponding distance for the monomer bond is obtained by adding the covalent radii of Ga and H ( $1.26 + 0.32 = 1.58 \text{ \AA}$ ).  $d_{\text{Ga-H}}$  for the bridging bond can be estimated by replacing the covalent radius of Ga by the average of the covalent and the atomic radii.

$$d_{\text{Ga-H}} = \frac{1.26 + 1.41}{2} + 0.32 = 1.65. \quad (2)$$

The larger bond length in the bridge, as compared with the monomer, lowers the force constants and thus the vibrational frequencies. We assume that this lowering is governed by the law  $\omega \sim d_{\text{Ga-H}}^{-4}$ , as corresponds to a typical mode Grüneisen parameter of 1.3. The lowering estimated according to this law does not suffice to explain the shift observed for the stretching vibrations, from  $1760 \text{ cm}^{-1}$  for the Ga-H monomer to  $1460$  for the bridging bond. The lowering needed can be accomplished by assuming that the bridging bonds are not colinear (see Fig. 11). The finite bond angle  $\theta$  produces a mixing of the bond stretching and the in-plane bond wagging (frequencies) according to the following equations:

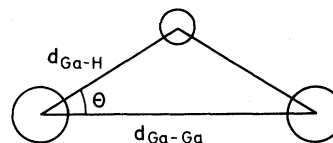


FIG. 11. Simple geometrical model for Ga—H—Ga bridging bond.

$$\omega_{\text{bs}}^2 = k_s^2 \omega_s^2 \cos^2 \theta + k_w^2 \omega_w^2 \sin^2 \theta, \quad (3a)$$

$$\omega_{\text{bw}_{\parallel}}^2 = k_s^2 \omega_s^2 \sin^2 \theta + k_w^2 \omega_w^2 \cos^2 \theta, \quad (3b)$$

where the subscripts bs and  $\text{bw}_{\parallel}$  refer to the stretching and in-plane wagging modes of the bridging hydrogen, respectively. The wagging mode which corresponds to a movement of the hydrogen atom perpendicular to the plane of Fig. 11 is unmixed and has a frequency

$$\omega_{\text{bw}_{\perp}} = k_w \omega_w. \quad (4)$$

The constants  $k_s$  and  $k_w$  ( $\leq 1$ ) represent the softening of the stretching and wagging restoring forces due to the increase in bond length. In the manner described above we estimate

$$k_s = (1.65/1.58)^{-4} = 0.84.$$

The frequencies  $\omega_s$  and  $\omega_w$  are taken to be those of the corresponding modes in the monomer bonds ( $\omega_s = 1760 \text{ cm}^{-1}$  and  $\omega_w = 565 \text{ cm}^{-1}$ ). We take, to a first approximation,  $k_s \simeq k_w = k$ , although as will be shown below,  $k_w$  is probably larger than  $k_s$ . From Eq. (3a) we obtain thus  $\theta = 10^\circ$ .

The width  $\Delta\omega$  of  $\omega_{\text{bs}}$  and  $\omega_{\text{bw}}$  can be accounted for by fluctuations in the angle  $\theta$  and the Ga-H distance  $d$  according to

$$2\omega_{\text{bs}}\Delta\omega_{\text{bs}} = k^2(\omega_w^2 - \omega_s^2)(\sin 2\theta)\Delta\theta + 2k(\omega_s^2 \cos^2 \theta + \omega_w^2 \sin^2 \theta) \frac{\partial k}{\partial d} \Delta d. \quad (5)$$

Similar calculation yields

$$|\Delta\omega_{\text{bw}_{\parallel}}| = |\Delta\omega_{\text{bs}}| (\omega_{\text{bs}}/\omega_{\text{bw}}).$$

TABLE III. Parameters of the Ga-H-Ga bands obtained from our model and from the experimental data.

	$\theta$	$k_s$	$k_w$	$d_{\text{Ga-H}}$	$d_{\text{Ga-Ga}}$
<i>a</i> -GaP:H	$7.9^\circ$	0.83	0.95	$1.65 \text{ \AA}$	$3.27 \text{ \AA}$
<i>a</i> -GaAs:H	$9.1^\circ$	0.84	0.94	$1.65 \text{ \AA}$	$3.26 \text{ \AA}$
<i>a</i> -GaSb:H	$9.6^\circ$	0.84	0.92	$1.65 \text{ \AA}$	$3.25 \text{ \AA}$

Experimentally we find  $\Delta\omega_{bs} \approx \pm 200 \text{ cm}^{-1}$ , and therefore  $\Delta\omega_{bw_{\parallel}} \approx \pm 600 \text{ cm}^{-1}$ , i.e., the in-plane wagging mode of the Ga—H—Ga bridges should be completely smeared out. In order to obtain a consistent interpretation of the data we must assume that this is indeed the case and that the  $\omega_{bw_{\parallel}}$  mode is not seen. The band at  $530 \text{ cm}^{-1}$  can then be assigned to the unmixed wagging vibration. The fact that this frequency is slightly lower than that of the monomer ( $565 \text{ cm}^{-1}$ ) corresponds to the fact that  $k_w$  is slightly higher than  $k_s$  ( $k_w \approx 0.94$ ).<sup>21</sup> The width of  $\omega_{bw}$  ( $\Delta\omega_{bw_{\perp}} \approx \pm 50 \text{ cm}^{-1}$ ) depends on  $d$  alone:

$$\Delta\omega_{bw_{\perp}} = \omega_w \frac{\partial K}{\partial d} \Delta d. \quad (6)$$

Equations (5) and (6) are solved simultaneously by  $\Delta d = \pm 0.05 \text{ \AA}$  and  $\Delta\theta = \pm 2^\circ$ .

The parameters  $k_s$  and  $k_w$  found from a fit of the experimental data for GaP, GaAs, and GaSb are listed in Table III. Included in this table are the angles  $\theta$  found with the corrected values of  $k_w$ .

We shall now make an attempt to estimate the hydrogen concentration in our *a*-GaAs:H from the integrated strength of the ir absorption bands. We recall, first of all, that the strength of the ir stretching bands due to bridging H bonds is believed to be much higher than that of the corresponding monomers.<sup>18</sup> This property is actually sometimes taken as a characteristic of the bridging bonds.<sup>18</sup> We believe that this fact is a peculiarity of the H bonds between atoms of the first period (B,C,N,O) and that it is actually due to the weakness of the monomer bond [a result of an accidental near-cancellation of the dynamical charge ( $e^* \approx 0.1$  for C—H) (Ref. 22)]. From the spectra of Ref. 23, for instance, we estimate for diborane  $e^* = 0.04$  for the stretching vibrations of the monomer B—H bonds and  $e^* = 0.6$  for those of the dimer bonds. The increase can be simply explained as related to the increase in polarity associated with the increase in bond length.<sup>24</sup>

We have listed in Table IV the integrated strengths  $\int [\alpha(\omega)/\omega] d\omega$  (in  $\text{cm}^{-1}$ ) of the observed infrared bands of several of our *a*-GaAs:H samples. These integrated strengths are related to the "transverse" effective charge  $e^*$  through<sup>12</sup>

$$\int \frac{\alpha d\omega}{\omega} = \frac{2\pi^2 N e^{*2}}{M c \omega_v}, \quad (7)$$

where  $\omega_v$  is the vibrational frequency,  $N$  the number per unit volume of the corresponding bonds

TABLE IV. Partial ( $N$ ) and total ( $C_H$ ) hydrogen concentrations for three different *a*-GaAs:H samples. The partial concentrations are calculated from the integrated strengths of the corresponding infrared absorption bands with the use of the proportionality constants given in the text. To calculate  $C_H$  (at. %), we used the atomic density of *c*-GaAs:  $4.4 \times 10^{22} \text{ cm}^{-3}$ .

$\omega$ ( $\text{cm}^{-1}$ )	2130	2040	1870	1760	1460	700	620	565	530	$\sum N_w$ ( $10^{21} \text{ cm}^{-3}$ )	$C_H^a$ (at. %)	$C_H^b$ (at. %)
	As-H <sub>2</sub>	As-H	Ga-H <sub>2</sub>	Ga-H	Ga-H-Ga	As-H <sub>2</sub>	As-H	Ga-H	Ga-H-Ga			
	str.	str.	str.	str.	str.	bend	wag	wag	wag			
$\int \frac{\alpha(\omega)}{\omega} d\omega$ ( $\text{cm}^{-1}$ )	1.9	4.0	2.9	8.7	282	5.5	23	37	143			
$N$ ( $10^{21} \text{ cm}^{-3}$ )						0.06	0.25	0.41	1.27	2.0	4.6	6.8
$\int \frac{\alpha(\omega)}{\omega} d\omega$ ( $\text{cm}^{-1}$ )	3.1	6.3	8.8	16.7	351	20	46	76	223			
$N$ ( $10^{21} \text{ cm}^{-3}$ )						0.22	0.51	0.84	2.0	3.7	8.4	10.7
$\int \frac{\alpha(\omega)}{\omega} d\omega$ ( $\text{cm}^{-1}$ )	7.8	15.2	21.2	38.6	487	27	68	113	310			
$N$ ( $10^{21} \text{ cm}^{-3}$ )						0.3	0.75	1.24	2.76	5.2	11.8	22.3

<sup>a</sup>From the integrated bond wagging absorptions.

<sup>b</sup>From  $N^{15}$  nuclear-reaction method.



and  $M$  the reduced mass (equal to the proton or deuteron mass). It is possible to evaluate  $N$  provided  $e^*$  is estimated in some way. If the same situation would prevail for Ga—H as for B—H (or C—H) the dominance of vibrations of Ga—H—Ga as compared with those of Ga—H would be due to a much larger  $e^*$  and not necessarily to a larger  $N$  for the bridging bonds. It is easy to convince oneself, however, that this is not the case. This follows simply when one considers that  $e^* \approx 0.35$  for the Ge—H bond<sup>22</sup> (about the same for the stretching as for the wagging vibrations). Hence  $e^*$  is much larger for GeH than for either B—H (0.04) or C—H (0.1). The effective charge for the Ga—H and the As—H bond are expected to be about the same because the effective dynamic charges in Ge and GaAs are the same.<sup>16</sup> In B—H or C—H we are thus dealing with a *suppression* of the monomer modes rather than an enhancement of the bridging modes.

The considerations above apply to molecules in gaseous form. For the solid form, one has to take into account local-field corrections and the fact that the refractive index  $n \neq 1$ . It is customary to write:

$$N_{s,w} = A_{s,w} \int \frac{\alpha}{\omega} d\omega. \quad (8)$$

It has been shown that the "constant"  $A_s$  for Ge—H stretching vibrations depends on  $N$  and on preparation conditions.<sup>25</sup> This is not the case for  $A_w$  which is equal to  $1.1 \times 10^{19} \text{ cm}^{-2}$ . Hence we take for the Ga—H and As—H bond:

$$\begin{aligned} A_w(\text{As—H}) &= A_w(\text{Ga—H}) = A_w(\text{Ge—H}) \\ &= 1.1 \times 10^{19}, \end{aligned} \quad (9)$$

in units of  $\text{cm}^{-2}$ . For the stretching vibrations of Ga—H—Ga, the effective charge must be increased so as to take into account the increased bond length. From Ref. 24 we estimate this increase in dynamical charge to be  $\sim 0.2$ . We hence take  $e^*(\text{Ga—H—Ga}) \sim e^*(\text{Ga—H}) + 0.2 = 0.55$ , and correspondingly (in units of  $\text{cm}^{-2}$ ),

$$\begin{aligned} A_w(\text{Ga—H—Ga}) &= 2A_w(\text{Ge—H}) \left[ \frac{0.35}{0.55} \right]^2 \\ &= 8.9 \times 10^{18}, \end{aligned} \quad (10)$$

where the factor of 2 accounts for the fact that one of the wagging modes is not seen due to the broadening discussed above.

We list in Table IV the values of  $H$  obtained for As—H, As—H<sub>2</sub>, Ga—H, Ga—H<sub>2</sub>, and Ga—H—Ga with the proportionality constants of Eqs. (9) and (10). The total concentration of H bonded to Ga and As are found to be 2.0 and  $3.7 \times 10^{21} \text{ cm}^{-3}$ , i.e., 4.6 and 8.4 at. %. These values agree acceptably with the total hydrogen concentration determined by the nuclear-reaction technique.<sup>25</sup> For the film with  $C_H = 22.3$  at. % we find a larger discrepancy: The ir data yield only half as much H as the nuclear-reaction method. This could be due to the presence of a corresponding fraction of nonbonded hydrogen in that particular specimen, although the uncertainties involved in the ir estimate do not allow for a firm conclusion.

The main conclusion from our present investigation is that hydrogen in amorphous III-V compounds is primarily bonded as bridging hydrogen in contrast to *a*-Si:H.<sup>12</sup> Finally, we would like to mention that about 70% of the hydrogen bonded in *a*-GaAs evolves at rather low temperatures ( $\sim 150^\circ\text{C}$ ). Our own measurements give about  $200^\circ\text{C}$  for this temperature. A connection between the low evolution temperature and the hydrogen bridges remains speculative, however.

#### ACKNOWLEDGMENTS

We would like to thank S. Kalbitzer for help with hydrogen-content measurement, R. Gibis and H. U. Habermeier for help with sample preparation, and M. Siemers and P. Wurster for their technical assistance.

\*On leave from Institute of Semiconductors, Chinese Academy of Sciences, Beijing, People's Republic of China.

<sup>1</sup>W. Paul, T. D. Moustakas, D. A. Anderson, and E. Freeman, *Proceedings of the Seventh International Conference on Amorphous and Liquid Semiconductors*,

edited by W. E. Spear (Edinburgh University, Edinburgh, 1977), p. 467.

<sup>2</sup>M. Hargreaves, M. J. Thompson, and D. Turner, J. Non-Cryst. Solids **35/36**, 403 (1980).

<sup>3</sup>D. K. Paul, J. Blake, S. Oguz, and W. Paul, J. Non-Cryst. Solids **35/36**, 501 (1980).

- <sup>4</sup>L. Alimoussa, H. Carchano, and J. P. Thomas, Ninth International Conference on Amorphous and Liquid Semiconductors, Grenoble, 1981 [J. Phys. (Paris) **42**, C4-683 (1981)].
- <sup>5</sup>M. Wihl, M. Cardona, and J. Tauc, J. Non-Cryst. Solids **8-10**, 172 (1972).
- <sup>6</sup>E. C. Freeman and W. Paul, Phys. Rev. B **20**, 716 (1979).
- <sup>7</sup>M. H. Brodsky, R. S. Title, K. Weiser, and G. D. Pettit, Phys. Rev. B **1**, 2632 (1970).
- <sup>8</sup>A. Heinemann, Ber. Bunsenges, Phys. Chem. **68**, 287 (1968).
- <sup>9</sup>D. Bermejo and M. Cardona, J. Non-Cryst. Solids **32**, 421 (1979).
- <sup>10</sup>A. P. Kurbakova, L. A. Leites, V. V. Garrilenko, X. Yu. N. Karuksin, and L. I. Zakharkin, Spectrochim. Acta **31A**, 281 (1975).
- <sup>11</sup>J. D. Odom, K. K. Chatterjee, and J. R. Durig, J. Phys. Chem. **84**, 1843 (1980).
- <sup>12</sup>M. H. Brodsky, M. Cardona, and J. J. Cuomo, Phys. Rev. B **16**, 3556 (1977).
- <sup>13</sup>H. Lüth and R. Matz, Phys. Rev. Lett. **46**, 1652 (1981).
- <sup>14</sup>H. Wagner, R. Butz, U. Backes, D. Bruchmann, Solid State Commun. **38**, 1155 (1981).
- <sup>15</sup>R. Fisch and D. C. Licciardello, Phys. Rev. Lett. **41**, 889 (1978).
- <sup>16</sup>W. A. Harrison, *Electronic Structure and the Optical Properties of Solids* (W. H. Freeman, San Francisco, 1979), p. 220.
- <sup>17</sup>P. R. Oddy and M. G. H. Wallbridge, J. Chem. Soc. Dalton, 572 (1978).
- <sup>18</sup>P. Schuster, G. Zundel, and C. Sandorfy, *The Hydrogen Bond* (North-Holland, Amsterdam, 1976), p. 299.
- <sup>19</sup>C. J. Buchenauer, M. Cardona, and F. H. Pollak, Phys. Rev. B **3**, 1243 (1971).
- <sup>20</sup>K. Steeples, G. Dearnaley, and A. M. Stoneham, Appl. Phys. Lett. **36**, 981 (1980). R. C. Newman and J. Woodhead, Radiat. Eff. **53**, 41 (1980).
- <sup>21</sup>M. I. Bell, Phys. Status Solidi B **53**, 675 (1972).
- <sup>22</sup>D. C. McKean, Chem. Commun. 147 (1966).
- <sup>23</sup>*Landolt-Börnstein Zahlenwerte und Funktionen, Band I, Teil 2* (Springer, Berlin, 1951), p. 355.
- <sup>24</sup>H. Müller, R. Trommer, M. Cardona, and P. Vogl, Phys. Rev. B **21**, 4879 (1980).
- <sup>25</sup>C. J. Fang, K. J. Gruntz, L. Ley, M. Cardona, F. J. Demond, G. Müller, and S. Kalbitzer, J. Non-Cryst. Solids **35**, 255 (1980); M. Milleville, M. Fuhs, F. J. Demond, H. Mannsperger, G. Müller, and S. Kalbitzer, Appl. Phys. Lett. **34**, 173 (1979).